

Statistical Inhomogeneity of Dates of Sudden Stratospheric Warmings in the Wintertime Northern Hemisphere

E. N. Savenkova^{a, *}, N. M. Gavrilov^{a, **}, A. I. Pogoreltsev^{b, ***}, and R. O. Manuilova^a

^a*St. Petersburg State University, St. Petersburg, 199034 Russia*

^b*Russian State Hydrometeorological University, St. Petersburg, 195196 Russia*

**e-mail: savenkova.en@mail.ru*

***e-mail: n.gavrilov@spbu.ru*

****e-mail: apogor@rshu.ru*

Received February 16, 2016; in final form, April 18, 2016

Abstract—Using the data of meteorological information reanalysis, a statistical analysis of dates of the main sudden stratospheric warmings observed in 1958–2014 has been performed and their inhomogeneous distribution in winter months with maximums in the beginning of January, from the end of January to the beginning of February, and in the end of February has been shown. To explain these regularities, a climatological analysis of variations in the amplitudes and vertical components of Eliassen–Palm fluxes created by large-scale planetary waves (PWs), as well as of zonal-mean winds and deviations of temperature from their winter-average values in high northern latitudes at heights of up to 50 km from the surface has been carried out using the 20-year (1995–2014) collection of daily meteorological information from the UK Met Office database. During the aforementioned intervals of observing more frequent sudden stratospheric warmings, climatological maximums of temperature perturbations, local minimums of eastward winds, and local maximums of the amplitude and Eliassen–Palm fluxes of PWs with a zonal wavenumber of 1 in the high-latitude northern stratosphere were found. Distinctions between atmospheric characteristics averaged over two last decades have been revealed.

Keywords: climatology, sudden stratospheric warming, zonal-mean wind, temperature, planetary waves, stratosphere dynamics

DOI: 10.1134/S0001433817030112

1. INTRODUCTION

Strong (up to 30–40 K) and fast increases in temperature in the wintertime polar stratosphere at heights of 30–50 km are known as sudden stratospheric warmings (SSWs) and occur mainly in the Northern Hemisphere. During major SSWs, reversals of stratospheric zonal fluxes take place.

Atmospheric perturbations related to SSWs can descend to the troposphere during time intervals from weeks to months [1] and produce significant weather phenomena, e.g., intense invasions of cold air in winter [2]. SSWs can have an effect on photochemical processes in the stratosphere [3], on the transfer of climatically active gases and contaminants [4, 5], and on the ozone variability in the Arctic and Antarctic regions [6].

From the date of the first discovered SSWs in 1952 [7], they are widely observed and classified by the World Meteorological Organization. The analysis involves, in particular, meteorological information reanalysis databases (see the survey in [8]) applicable for studying climatic changes [9]. In [10], the NCEP/NCAR and ERA meteorological reanalysis databases were used, different methods of identifying SSWs were applied, and dates of main SSWs observed

in 1958–2013 were tabulated. When considering these tables, there appears a hypothesis that dates of main SSWs can be inhomogeneously distributed in winter months and there can exist climatologically preferable intervals of occurrence of these phenomena.

To verify this hypothesis, analysis of climatological atmospheric characteristics related to the development of SSWs is carried out in this investigation using 20-year (1995–2014) collections of daily meteorological data in the assimilation system of the United Kingdom Met Office (UKMO) [11] at heights of up to 50 km. We have analyzed amplitudes and Eliassen–Palm fluxes (EP fluxes) created by modes of planetary waves (PWs) with zonal wavenumbers $m = 1$ and 2, as well as the longitude-average zonal wind and temperature deviations from winter-average values at heights of up to 50 km from the Earth's surface. These climatic data were compared with results of the statistical analysis of observed dates of main SSWs.

2. METHODS AND DATA

The climatic 20-year average atmosphere characteristics responsible for the formation of SSWs were

obtained using daily values of meteorological variables from the UKMO meteorological reanalysis database [11] for the winter month (from December to February) of 1995–2014 in the height range of 0–50 km. For the aforementioned interval, the zonal wind and deviations of temperature from its winter-average values were calculated and averaged. To obtain parameters of PWs responsible for SSWs, the Fourier analysis was performed with the decomposition of hydrodynamic variables into zone-average values and superposition of harmonics with zonal wavenumbers $m = 1-4$; below they are called PW1–PW4.

Mechanisms of the SSW formation are often analyzed using Eliassen–Palm fluxes which characterize the PW energy [12]. The EP-flux vector represents the zonal-mean direction of wave activity propagation in the meridional plane. The meridional and vertical components of the EP-flux include heat and momentum fluxes created by PWs. In this study, climatological mean values of the vertical component of EP fluxes for PWs with zonal wavenumbers 1 and 2 were found using the usual formula [13]

$$F_z = \rho_0 a \times \cos \varphi \left\{ \left[f - \frac{1}{a \cos \varphi} \frac{\partial}{\partial \varphi} (\bar{u} \cos \varphi) \right] \frac{\overline{v'\theta'}}{\bar{\theta}_z} - \overline{w'u'} \right\}, \quad (1)$$

where a and f are the Earth's radius and Coriolis parameter, respectively; ρ_0 is the background density; φ is the latitude; u , v , and w are the zonal, meridional, and vertical components of the wind, respectively; and θ is the potential temperature. The overbar and primes denote zonal-mean values and deviations from them, respectively.

3. RESULTS

In what follows, the climatology of SSW dates and associated atmospheric characteristics are studied by data of reanalysis of the UK Met Office meteorological information for winter seasons of 1995–2014.

3.1. Statistics of SSW Dates

Figure 1 shows 20-year averaged amplitudes and vertical components of the EP flux for PW1 and PW2, zonal-mean wind, and deviation of temperature from its winter-average values for every day in December–February in middle and high latitudes of the Northern Hemisphere. The descending cold and warm layers shown in Fig. 1f reflect seasonal changes in temperature at heights of up to 50 km caused by the decrease in the surface temperature to its minimum in January–February and seasonal variations in radiation heat inflows and circulation in the stratosphere during the polar night. Studying height–latitude distributions of monthly average temperatures at heights of 5–35 km by data of the low-orbit CHAMP GPS satellite [14, 15] shows considerable minimums of temperature at

heights above 30 km near the North Pole in November–December. Then, these minimums become less deep and descend by analogy with Fig. 1f. The maximums in the zone of positive temperature deviations in Fig. 1f become stronger below 40 km, where main SSWs often occur.

Inside the warmer layer in Fig. 1f, in addition to seasonal variations, one can see local temperature maximums in the beginning of January, from the end of January to the beginning of February, and in the end of February. These maximums can reflect the SSW contribution averaged over 20 years. The presence of several local maximums in Fig. 1f suggests that SSW dates can be distributed inhomogeneously with a higher frequency of occurrence of warmings in certain intervals of dates in January–February.

To verify the hypothesis about the inhomogeneous distribution of SSW dates during winter, dates of all stratospheric warmings were determined, including the main (major) and weaker (minor) ones we found in the reanalysis database of the UKMO meteorological information during 1995–2014. We used the standard SSW definition (an increase in temperature and weakening or reversal of the zonal wind in polar latitudes [10]), but took a wider height interval of up to 50 km. The table presents the number of major and minor SSWs recorded in subsequent 10-day intervals during winter. Since the total number of SSWs recorded in 1995–2014 is not very large, we completed the table with numbers of dates of major SSWs that were accompanied by the zonal wind reversal and identified during 1958–2013 [10] using different methods and NCAR/NCEP meteorological reanalysis database. We also added numbers of SSWs in 1980–1995 from the MERRA meteorological reanalysis database developed by NASA in the United States [16].

For the last row of the table, probabilities of the hypothesis about the homogeneous distribution of SSW dates were determined using the χ^2 statistical test [17]. This probability turned out to be less than 0.01, which justifies the inhomogeneity of the SSW date distribution in winter time intervals shown in the table. The SSW number distribution in the last row of the table has local maximums in the beginning of January, from the end of January to the beginning of February, and in the end of February. To verify the significance of these local maximums, additional χ^2 tests for the homogeneity of the probability distributions of dates inside fragments of the last row of the table were carried out. The fragments consisted of 2–4 intervals and contained neighboring maximum and minimum values of the SSW numbers. For the abovementioned three local maximums in the last row of the table, probabilities of accepting the hypotheses of homogeneity in their neighborhoods do not exceed 0.03–0.07. This gives grounds to believe that the maximums of recorded SSW events in the last row of the table are significant.

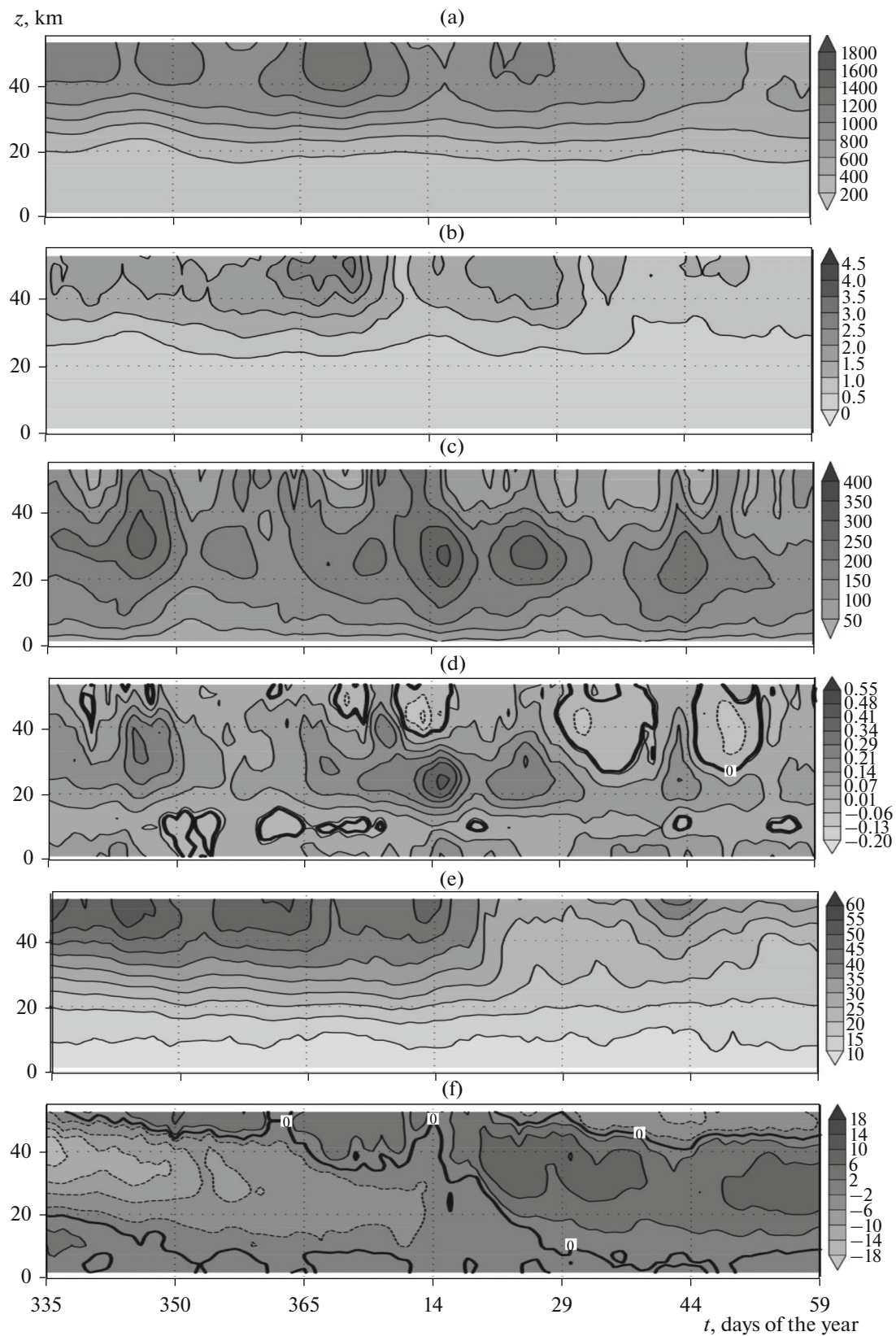


Fig. 1. (a) Amplitude of variations in the geopotential height in PW1, gpm (averaged for 1995–2014); (b) vertical PW1 EP-flux, $\text{s m}^{-1} \text{kg}^{-2}$; (c) amplitude of geopotential height variations in PW2, gpm; (d) vertical PW2 EP-flux, $\text{s m}^{-1} \text{kg}^{-2}$; (e) longitude-averaged zonal wind, m/s; and (f) deviation of temperature from its winter-average value, K. Plots (a)–(e) were constructed for 62°N and plot (f) for 87.5°N . The solid lines denote lines of zero values.

Numbers of SSWs identified in subsequent 10-year intervals (with days of the years) and total numbers N according to reanalyzed meteorological information of MERRA in 1980–1994, UKMO in 1995–2014, and NCEP/NCAR for 1958–2013 [10]

Data and years	N	December			January			February		
		336–345	346–355	356–365	1–10	11–20	21–30	31–40	41–50	51–60
MERRA, 1980–1994	20	1	0	0	3	0	6	3	3	4
UKMO, 1995–2014	40	1	4	3	6	3	8	6	4	5
NCAR/NCEP, 1958–2013	55	5	2	4	10	5	8	7	3	11
Totally, 1958–2014	115	7	6	7	19	8	22	16	10	20

The aforementioned intervals (the beginning of January, the end of January—the beginning of February, and the end of February) coincide with the position of local temperature maximums in Fig. 1f and corroborate that the statistical probability of recording SSWs is higher within the aforementioned periods.

3.2. Average Atmosphere Characteristics Related to SSWs

To determine the causes of the inhomogeneity found above in the SSW date distribution, the climatology of atmosphere characteristics having an effect on the SSW formation (see Section 2) was analyzed.

In Fig. 1a, local maximums of 20-year averaged PW1 amplitudes with a principal maximum in the beginning of January at heights of 40–50 km are seen. Then, local maximums of PW1 amplitudes in Fig. 1a decrease due to seasonal variations in the mean zonal wind and intensity of planetary wave sources. The abovementioned maximum values of the amplitudes correspond to maximums of vertical EP fluxes for PW1 in Fig. 1b. These fluxes are positive almost everywhere and correspond to the propagation of PW1 wave activity upward from wave sources in lower layers of the atmosphere. Positive values of the vertical component of the EP flux in Fig. 1b correspond to zonal-mean meridional heat fluxes created by PW1 in the direction of the North Pole. This corroborates the existing ideas [18, 19] according to which an important cause of SSWs is the heating of polar regions by heat advection from planetary waves. The heating weakens the polar vortex and decreases its eastward velocity.

Maximums of 20-year average amplitudes of PW1 EP fluxes in Figs. 1a and 1b occur after corresponding local maximums of the 20-year averaged zonal wind shown in Fig. 1e; last maximums of the amplitude and EP fluxes of PW1 stronger are retarded with respect to corresponding maximums of the wind velocity. The quasi-periodic variations in the mean wind and PW amplitudes with periods of 1–4 weeks are supposed to be caused by the so-called vacillations occurring due to changes in the PW propagation conditions and nonlinear interactions between PWs and mean wind [18, 20]. The intensity and duration of these vacillations change from year to year. In the case of uniform random distri-

bution of vacillation phases, one should expect full smoothing of local maximums and minimums in Figs. 1a, 1b, and 1e. The presence of local maximums in these figures can testify to the existence of vacillation phases repeating in different years.

Figures 1c and 1d present 20-year average amplitudes and vertical components of the EP flux for PW2, respectively. In Fig. 1d, local regions of negative (downward directed) vertical EP fluxes of the PW2 mode are revealed. They can be caused, e.g., by reflection of PW2 propagating from below or by the generation of the PW2 mode at heights of the middle atmosphere. The relative magnitudes and dimensions of regions of negative EP fluxes are less than for positive fluxes in Fig. 1d. Negative EP fluxes in Fig. 1d correspond to the wave heat transfer to the south and additional cooling of the middle atmosphere near the North Pole.

Main climatological maximums of the PW2 amplitude in Fig. 1c are positioned at heights of about 30 km, which are significantly less than heights of maximums of PW1 amplitudes (40–50 km in Fig. 1a). This can be caused by a stronger effect of the mean wind on the refractive index for PW2, which impedes the PW2 propagation to the region of strong eastward winds. A numerical simulation of height–latitude distributions of amplitudes of different PW modes [21] demonstrated the presence of a maximum of the stationary PW2 amplitude at heights of 30–40 km in high latitudes of the wintertime Northern Hemisphere. In the middle of January, Fig. 1c shows the largest PW2 amplitude. Numerical calculations [22] revealed the presence of vacillations with counterphase changes in the PW1 and PW2 amplitudes in the stratosphere. The principal maximums of the PW2 amplitudes and EP fluxes in Figs. 1b and 1c are positioned mainly between the corresponding maximums of PW1 amplitudes and EP fluxes in Figs. 1a and 1b, which does not contradict the calculations [22]. This suggests the energy exchange between PW1 and PW2 due to the nonlinear wave interaction. For some local PW2 maximums in Figs. 1c and 1d, their phase opposition to PW1 maximums in Figs. 1a and 1b is not expressed sufficiently clearly. This can be related to PW phase differences between heights of principal maximums of PW1 (40–50 km) and PW2 (30–40 km), as well as to

the existence of other mechanisms having an effect on the PW2 propagation in the middle atmosphere.

Climatological 20-year average zonal wind velocities in Fig. 1e exceed 30 m/s (with maximums of up to 55 m/s) at heights above 30 km before the end of January and become less than 30 m/s after January 20–25. These intervals coincide with time points when the lower boundary of the warm zone in Fig. 1f crosses heights of 20–25 km and the polar stratosphere warms up. In the middle of February, the 20-year zonal-mean wind at heights of 40–50 km in Fig. 1e again rises for a week or two. During this time, the polar stratosphere cools down (see Fig. 1f), which can favor the increase in the circumpolar vortex.

A comparison of intervals with more frequent SSW events in the beginning of January, from the end of January to the beginning of February, and in the end of February in the table with Figs. 1a and 1b reveals the presence of local maximums of PW1 amplitudes and EP fluxes in the aforementioned intervals (for the last interval, a considerable separation of the local maximums of the PW1 EP flux and amplitude is observed in Figs. 1a and 1b). All three intervals of higher SSW activity correspond to the decrease in climatological zonal-mean eastward winds in Fig. 1e. Thus, the more frequent occurrence of SSWs in the aforementioned time intervals can be explained by the existence of the above-discussed repeating phases of PW vacillations and mean wind in different years.

3.3. Decade Variations in Climate Characteristics

To analyze possible changes in conditions of SSW development in the stratosphere, we divided the 20-year interval of UKMO data into two subgroups of 10 years. Figures 2 and 3 are similar to Fig. 1 but present atmosphere characteristics averaged over two 10-year intervals, 1995–2004 and 2005–2014, respectively. The configuration of height zones of positive and negative temperature deviations in Fig. 3f is in general similar to Fig. 1f. However, in Fig. 2f for 1995–2004, the warm layer descends faster in the beginning of winter and then is interrupted at a height of 30–40 km. The main maximums of temperature deviations in Fig. 2f are weaker than in Fig. 3f. The differences between Figs. 2f and 3f reflect the climatological variability of the stratosphere temperature structure in different decades.

A comparison of Figs. 2f and 1f shows that the polar atmosphere at heights of 30–50 km from the end of December to the beginning of January in 1995–2004 was warmer than its 20-year mean climatological state. This caused weakening of the circumpolar vortex in the beginning of winter and the formation of the zonal wind minimum to 30 m/s in 1995–2004 in Fig. 2e. The cooling of the polar atmosphere at heights of 30–50 km in the middle of January (Fig. 2f) accelerates the zonal mean flux (Fig. 2e). Temporary variations in the zonal-mean eastward wind in Fig. 3e in 2005–2014

are similar to those in Fig. 1e for climatological 20-year means. It is interesting that considerable regions of negative PW2 EP-fluxes are revealed from the end of December to the beginning of January in 1995–2005 in Fig. 2d. These fluxes correspond to meridional wave heat fluxes to the South, which creates additional cooling of the polar middle atmosphere.

Figures 2a–2d and 3a–3d represent 10-year average amplitudes and vertical components of EP-fluxes for PW1 and PW2, respectively. In 2005–2014, height–time variations in Figs. 3a–3d are mainly similar to corresponding variations in 20-year means presented in Figs. 1a–1d. In 1995–2004, the aforementioned distinctions in temperature and zonal wind in Figs. 2e and 2f lead to distinctions in Figs. 2a–2d as compared to Figs. 1a–1d. The main maximum of PW1 amplitudes and EP-fluxes in Figs. 2a and 2b displaces from the beginning of January to the end.

Distinctions in atmospheric characteristics shown in Figs. 2 and 3 during the last two decades demonstrate significant changes in the climatological regime of the wintertime polar middle atmosphere. The maximum PW1 amplitudes are greater by 400–600 gpm in upper layers of the stratosphere in 2005–2014. In these years, maximum PW2 amplitudes increase and propagate to heights of 40–50 km (Fig. 3c). A comparison of 10-year average deviations of temperature in Figs. 2f and 3f reveals stronger heating of the polar stratosphere in 2005–2014. This, in turn, leads to more frequent weakenings (destructions) of the polar vortex in the middle of winter during the last decade. Revealing whether the described 10-year distinctions reflect stable trends or temporary changes in the climatic system requires further observations.

4. CONCLUSIONS

In this work, statistical analysis of SSW dates identified by reanalyzed meteorological information from UKMO in 1995–2014 and NCAR/NCEP in 1958–2014 has been carried out. It was found that the distribution of the SSW number in winter is inhomogeneous and has three maximums of SSW probability in the beginning of January, from the end of January to the beginning of February, and in the end of February.

The climatology of atmosphere parameters related to SSWs has been analyzed by data of the 20-year (1995–2014) series of daily assimilation of UKMO meteorological data. Amplitudes and EP fluxes for PW modes with zonal wavenumbers $m = 1$ and 2, zonal-mean wind, and deviations of temperature from its winter-average values in high northern latitudes at heights of up to 50 km from the Earth's surface have been analyzed.

Average temperature deviations for 20 years exhibit cold and warm layers descending during winter and related to seasonal variations during the polar night. Average amplitudes and vertical components of the EP

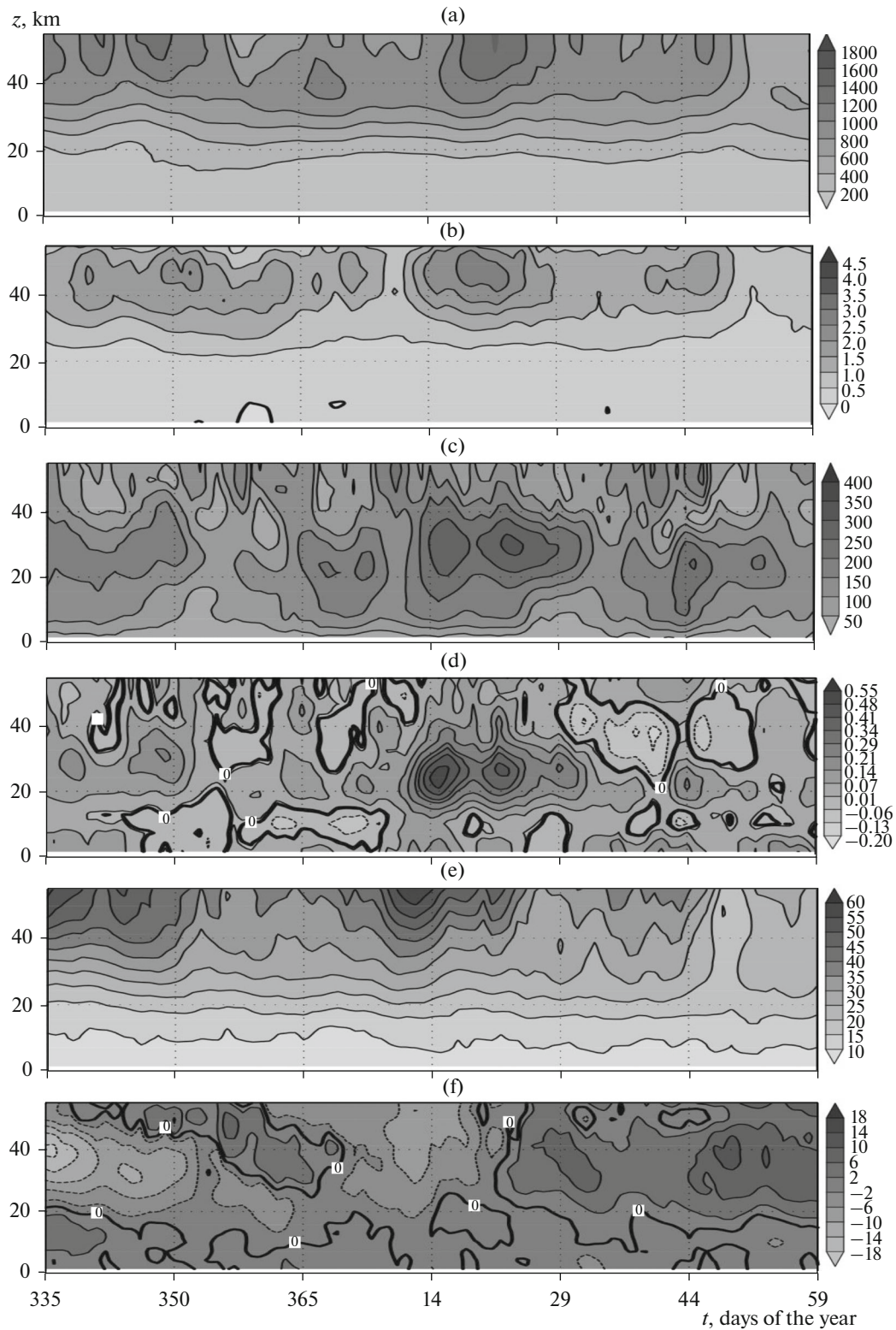


Fig. 2. Same as in Fig. 1 but for 1995–2004.

flux for 20 years have quasi-periodic increases with main maximums in the beginning of January at heights of 40–50 km. Main climatological maximums

of amplitudes and upward EP fluxes are at much lower heights (about 30 km), with the largest maximum in the middle of January. Differences between atmo-

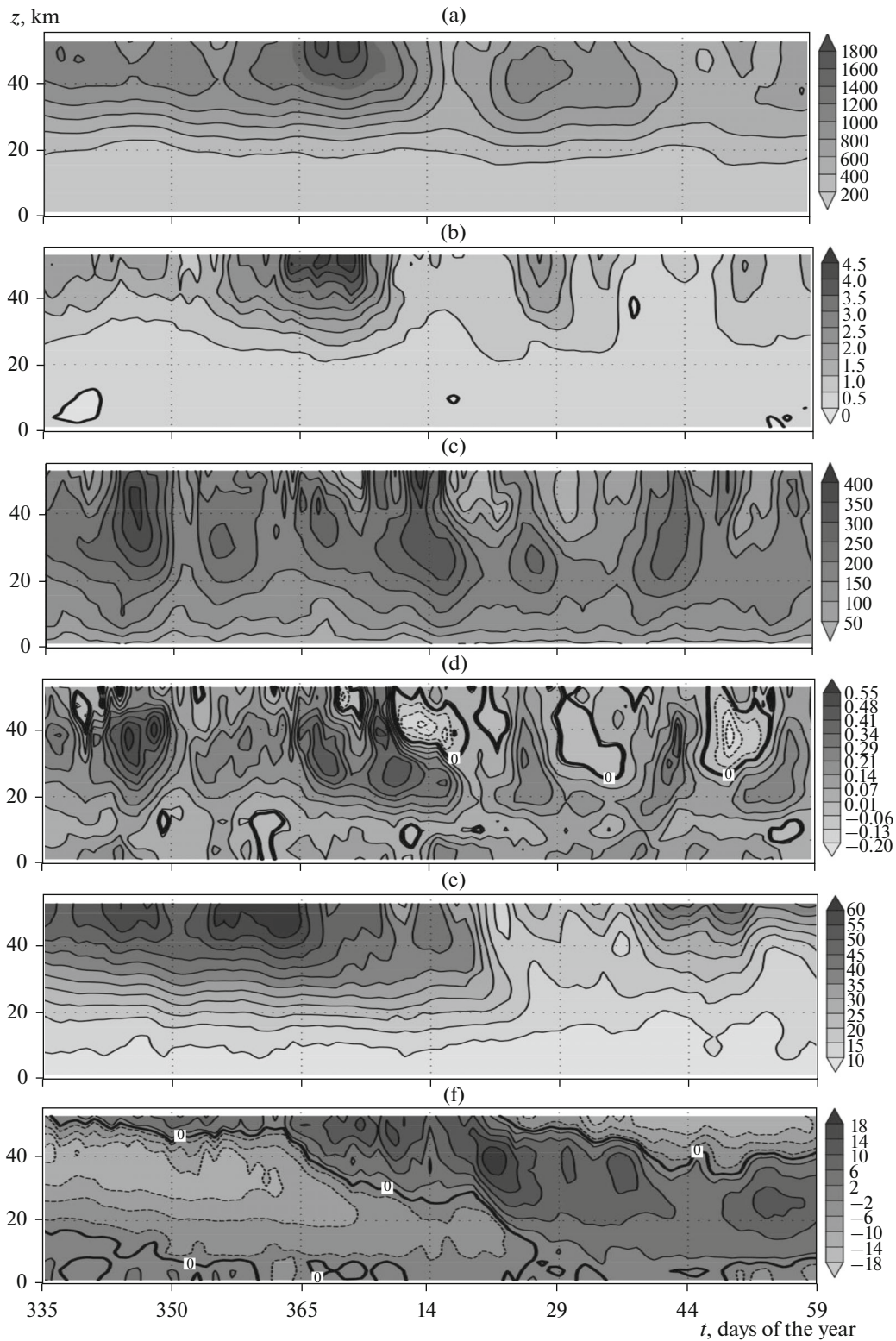


Fig. 3. Same as in Fig. 1 but for 2005–2014.

sphere characteristics averaged over the last two decades (1995–2004 and 2005–2014) are observed. They include an increase in the maximum amplitudes

and EP fluxes for PW1 and PW2, as well as a weakening of eastward winds and warming of the polar stratosphere during 2005–2014.

The aforementioned intervals of maximum probability of the SSW appearance coincide with climatologic maximums of temperature deviations, minimums of eastward winds, and maximums of amplitudes of EP fluxes for PW1. They can be caused by vacillation phases of the mean wind and PW amplitudes repeating in different years.

Revealing whether the climatic distinctions observed in recent decades reflect stable trends or short-time variability of the atmospheric climatic system requires further investigations.

ACKNOWLEDGMENTS

We are grateful to the British Atmospheric Data Centre and NASA (United States) for access to assimilation data of the UK Met Office and MERRA meteorological information. This work was supported by the Russian Science Foundation, project no. 14-17-00685.

REFERENCES

1. M. P. Baldwin and T. J. Dunkerton, "Stratospheric harbingers of anomalous weather regimes," *Science* **294**, 581–584 (2001). doi 10.1126/science.1063315
2. D. W. J. Thompson, M. P. Baldwin, and J. M. Wallace, "Stratospheric connection to Northern Hemisphere wintertime weather: Implications for prediction," *J. Clim.* **15**, 1421–1428 (2002). doi 10.1175/1520-0442(2002)015<1421:SCTNHW>2.0.CO;2
3. G. L. Manney, J. L. Sabutis, S. Pawson, M. L. Santee, B. Naujokat, R. Swinbank, M. E. Gelman, and W. Ebisuzaki, "Lower stratospheric temperature differences between meteorological analyses in two cold Arctic winters and their impact on polar processing studies," *J. Geophys. Res.: Atmos.* **108**, 8328 (2003). doi 10.1029/2001JD001149
4. X. Jiang, J. Wang, E. T. Olsen, T. Pagano, L. L. Chen, Y. L. Yung, "Influence of stratospheric sudden warming on AIRS mid-tropospheric CO₂," *J. Atmos. Sci.* **70**, 2566–2573 (2013). doi 10.1175/JAS-D-13-064.1
5. A. H. Butler, L. M. Polvani, and C. Deser, "Separating the stratospheric and tropospheric pathways of El Niño–Southern Oscillation teleconnections," *Environ. Res. Lett.* **9**, 024014 (2014). doi 10.1088/1748-9326/9/2/024014
6. M. Schoeberl and D. Hartmann, "The dynamics of the stratospheric polar vortex and its relation to springtime ozone depletions," *Science* **251**, 46–52 (1991). doi 10.1126/science.251.4989.46
7. R. Scherhag, "Die explosionsartigen Stratosphärenwärmungen des Spätwinters 1952," *Ber. Dtsch. Wetterdienstes* **38**, 51–63 (1952).
8. K. G. Rubinshtein and A. M. Sterin, "Comparison of reanalysis products and aerological data," *Izv., Atmos. Ocean. Phys.* **38** (3), 264–276 (2002).
9. V. M. Khan, A. M. Sterin, and K. G. Rubinshtein, "Estimates for temperature trends in the free atmosphere according to reanalysis and radiosonde observation data," *Meteorol. Gidrol.* **28** (12), 5–18 (2003).
10. A. Butler, D. Seidel, S. Hardiman, N. Butchart, T. Birner, and A. Match, "Defining sudden stratospheric warmings," *Bull. Am. Meteorol. Soc.* **96** (11), 1913–1928 (2015). doi 10.1175/BAMS-D-13-00173.1
11. R. Swinbank and A. O'Neill, "A stratosphere–troposphere data assimilation system," *Mon. Weather Rev.* **122**, 686–702 (1994).
12. D. G. Andrews, J. R. Holton, and C. B. Leovy, *Middle Atmosphere Dynamics* (Elsevier, New York, 1987).
13. M. Inoue, M. Takahashi, and H. Naoe, "Relationship between the stratospheric quasi-biennial oscillation and tropospheric circulation in northern autumn," *J. Geophys. Res.* **116**, D24115 (2011). doi 10.1029/2011JD016040
14. N. M. Gavrilov, "Structure of the mesoscale variability of the troposphere and stratosphere found from radio refraction measurements via CHAMP satellites," *Izv., Atmos. Ocean. Phys.* **43** (4), 492–501 (2007).
15. N. M. Gavrilov, "Monthly height–latitude distributions of temperature mesoscale variances at altitudes 0–35 km in years 2001–2005 from CHAMP GPS satellite data," ResearchGate, Dataset 2007. doi 10.13140/RG.2.1.3214.7046
16. M. M. Rienecker, M. J. Suarez, R. Gelaro, R. Todling, J. Bacmeister, E. Liu, M. G. Bosilovich, S. D. Schubert, L. Takacs, G.-K. Kim, S. Bloom, J. Chen, D. Collins, A. Conaty, and A. Silva, "MERRA: NASA's modern-era retrospective analysis for research and applications," *J. Clim.* **24**, 3624–3648 (2011). doi 10.1175/JCLI-D-11-00015.1.2011
17. J. A. Rice, *Mathematical Statistics and Data Analysis* (Duxbury Press, Belmont, 2006).
18. J. R. Holton and C. Mass, "Stratospheric vacillation cycles," *J. Atmos. Sci.* **33**, 2218–2225 (1976).
19. A. I. Pogoreltsev, E. N. Savenkova, O. G. Aniskina, T. S. Ermakova, W. Chen, and K. Wei, "Interannual and intraseasonal variability of stratospheric dynamics and stratosphere–troposphere coupling during northern winter," *J. Atmos. Sol.–Terr. Phys.* **136**, 187–200 (2015). doi 10.1016/j.jastp.2015.08.008
20. R. A. Plumb, "Planetary waves and the extratropical winter stratosphere," *Geophys. Monogr. Ser.* **190**, 23–41 (2010). doi 10.1029/2009GM000888
21. N. M. Gavrilov, A. V. Koval, A. I. Pogoreltsev, and E. N. Savenkova, "Simulating influences of QBO phases and orographic gravity wave forcing on planetary waves in the middle atmosphere," *Earth, Planets Space* **67**, 86 (2015). doi 10.1186/s40623-015-0259-2
22. W. A. Robinson, "A model of the wave 1–wave 2 vacillation in the winter stratosphere," *J. Atmos. Sci.* **41** (21), 2289–2304 (1985).

Translated by A. Nikol'skii